

**APPLICATIONS OF LDPC CODES FOR HYBRID
WIRELESS OPTICAL AND MAGNETIC RECORDING
SYSTEMS**

A Thesis Presented

by

SARMA VANGALA

Submitted to the Graduate School of the
University of Massachusetts Amherst in partial fulfillment
of the requirements for the degree of

MASTER OF SCIENCE IN ELECTRICAL AND COMPUTER ENGINEERING

September 2007

Electrical and Computer Engineering

**APPLICATIONS OF LDPC CODES FOR HYBRID
WIRELESS OPTICAL AND MAGNETIC RECORDING
SYSTEMS**

A Thesis Presented

by

SARMA VANGALA

Approved as to style and content by:

Hossein Pishro-Nik, Chair

Dennis Goeckel, Member

Patrick Kelly, Member

Christopher Hollot, Department Chair
Electrical and Computer Engineering

To Amma, Nanna and Siri.

ABSTRACT

APPLICATIONS OF LDPC CODES FOR HYBRID WIRELESS OPTICAL AND MAGNETIC RECORDING SYSTEMS

SEPTEMBER 2007

SARMA VANGALA

B.Tech., JNT UNIVERSITY COLLEGE OF ENGINEERING

M.S.C.S., UNIVERSITY OF SOUTH FLORIDA

M.S.E.C.E., UNIVERSITY OF MASSACHUSETTS AMHERST

Directed by: Professor Hossein Pishro-Nik

This thesis comprises of two parts. In the first, we improve the performance of existing hybrid FSO/RF communication systems. Conventional hybrid RF and optical wireless communication systems make use of independent and parallel Free Space Optical (FSO) and RF channels to achieve higher reliability than individual channels. This thesis is based on the idea that true hybridization can be accomplished only when both channels collaboratively compensate the shortcomings of each other and thereby, improve the performance of the system as a whole. We believe that optimization on the combined channel capacities instead of the individual channel capacities of the FSO and RF channels can increase the system availability by a large amount. Using analysis and simulation, we show that, by using Hybrid Channel Codes, we can obtain more than two orders of magnitude improvement in bit error rates and many-fold increase in system availability over the currently existing best systems.

Simulations also show that the average throughput obtained using the new system is over 35% better when compared to the present systems. The goodput is much higher because of the elimination of data repetition. Also by avoiding data duplication, we preserve to a great extent the crucial security benefits of FSO communications.

The second half of the thesis deals with magnetic recording systems. Due to the insatiable and ever-increasing needs of data storage, novel techniques have to be developed to improve the capacity of magnetic recording channels. These capacity requirements translate to improving storage densities and using higher recording rates. For these channels, improvements even in the order of a tenths of a dB have a big impact on the storage densities of the recording device. Recently, LDPC codes have been constructed to achieve the independent and uniformly distributed (i.u.d.) capacity of partial response (PR) channels. The “guess algorithm” has been proposed for memoryless channels, to improve the performance of iterative belief propagation decoding to that of Maximum Likelihood (ML) decoding. In the second part of this thesis, the “guess algorithm” is extended to channels with memory. It is shown using asymptotic density evolution analysis that the gains obtained using this algorithm on these channels are more than those obtained over memoryless channels. The “guess algorithm” is further extended to magnetic recording channels which are characterized by ISI and additive white gaussian noise (AWGN). Simulations show that gains of upto a dB are possible on magnetic recording channels.

TABLE OF CONTENTS

	Page
ABSTRACT	iv
LIST OF TABLES	viii
LIST OF FIGURES	ix
 CHAPTER	
1. INTRODUCTION	1
1.1 Error Control Coding and LDPC Codes	1
1.2 Contributions of Thesis	2
1.2.1 Hybrid FSO/RF Communication Systems	2
1.2.2 Improved Decoding Algorithm on Channels with Memory	3
1.3 Outline of Thesis	3
2. HYBRID RF OPTICAL WIRELESS NETWORKS	5
2.1 Introduction	5
2.2 Related Work	6
2.3 A Novel Hybrid FSO/RF System	9
2.3.1 Channel Model	9
2.3.2 Definitions and Notations	11
2.3.3 Case 1: Fixed Rate Code on a Single FSO Link	12
2.3.4 Case 2: Adaptive Rate Codes on a Single FSO Link	12
2.3.5 Case 3: RF Backup Channel with a Fixed Rate Code	13
2.3.6 Case 4: RF Backup Channel with Adaptive Codes	13
2.3.7 Case 5: Independent Parallel FSO/RF Channels with Adaptive Codes	14
2.3.8 Case 6: Hybrid Channel Codes for Combined FSO/RF Channels	14

2.4	A Novel Coding Mechanism	16
2.4.1	Hybrid Channel Codes	17
2.4.2	Optimality of Hybrid Channel Codes for Hybrid FSO/RF Channels	19
2.4.3	Density Evolution	22
2.4.4	Achievable Rate Region for Iterative Decoding	23
2.5	Performance Results	25
2.5.1	Simulation Setup	25
2.5.2	Results	26
2.5.2.1	Comparison of Channel Utilization for Various Coding Schemes	26
2.5.2.2	Comparison of System Availability	29
2.5.2.3	Comparison of Bit Error Rates for various Coding Schemes	29
2.6	Broader Impacts	31
3.	IMPROVED DECODING ALGORITHM ON CHANNELS WITH MEMORY	32
3.1	Introduction	32
3.2	Related Work	33
3.3	Improved Decoding Algorithm for ISI Channels	35
3.4	Density Evolution on ISI Channels	37
3.5	Simulation Results	39
3.6	Summary and Future Work	44
4.	CONCLUSIONS	45
	BIBLIOGRAPHY	47

LIST OF TABLES

Table	Page
2.1 Simulation parameters used for various channel conditions.	26
2.2 Comparison of goodputs (in Gbps)obtained for various FSO systems.	29
2.3 Comparison of channel availability for combined and independent FSO/RF systems.	29
3.1 Density evolution analysis of improved decoding over AWGN channels.	42
3.2 Density evolution analysis of improved decoding over ISI channels with AWGN.	42

LIST OF FIGURES

Figure	Page
2.1 System availability for different optical wireless systems.	16
2.2 Graphical representation of Hybrid Channel Codes.	18
2.3 Hybrid Channel Coding architecture.	19
2.4 Proof of Theorem 1.	20
2.5 The achievable region for the puncturing pair $[p_{RF}, p_{FSO}]$	24
2.6 Simulation setup.	26
2.7 Code rate variation for different FSO/RF systems.	27
2.8 BER performance of different optical wireless systems.	30
3.1 Block Diagram of PR channel	36
3.2 Equivalent channel for the improved decoding.	39
3.3 Improved performance using the guess algorithm for block length 1000 on a dicode channel.	41
3.4 Improved performance using the guess algorithm for block length 4096 on a dicode channel.	43
3.5 Improved performance using the guess algorithm for various PR channels for block length 1000.	43

CHAPTER 1

INTRODUCTION

1.1 Error Control Coding and LDPC Codes

In today's "networked" world, reliable transmission of a message is of utmost importance. With his pioneering paper [45], Shannon laid the foundations for information and coding theory in the late 1940s. Since then, the world of information theory and digital communications has grown tremendously; with applications in nearly every walk of life. Using error correcting codes, transmission errors can be corrected using clever mathematical techniques. This is called channel coding. Codes can also be used to reduce the number of bits needed to represent the original data, called source coding. In this thesis, we deal with channel coding techniques for two important communication systems. We show that using efficient applications of channel coding techniques in these systems, we can improve their performance in many ways and make them practical for application in the real world.

Many coding techniques have been proposed in the last 60 years. Of these, linear block codes with their simplicity of design and ease for analysis, have occupied a major role in communication and information theory. Though invented in 1960s, Low Density Parity Check Codes (LDPC) [15] were not utilized until the recent past due to the enormous computational complexities involved. However, due to the recent advances in technology, LDPC codes have been found to exhibit extremely useful applications in most channels of practical interest [31, 30, 29]. These codes are now being used to improve the performance of many communication systems. In particular, LDPC codes use sparse generator matrices that can make encoding easier

[6]. Also, LDPC codes use iterative decoding algorithms that are linear in complexity unlike previous decoding techniques [31]. In this thesis, we apply LDPC codes to two important systems: the hybrid FSO/RF communication system and the magnetic recording system. We believe that significant gains, in terms of bandwidth utilization and system availability, in case of hybrid FSO/RF networks and, storage densities, in case of magnetic recording systems can be obtained using the improvements suggested in this work.

1.2 Contributions of Thesis

The thesis contributes to the areas of hybrid FSO/RF communication systems and magnetic recording systems. In both these areas, the contributions provided by this thesis help improve the performance of the respective communication system in terms of utilization of the channel resources and improved performance over existing systems.

1.2.1 Hybrid FSO/RF Communication Systems

To the area of hybrid FSO/RF communication systems, this work contributes the following.

- A novel look at the hybrid FSO/RF systems based on the combined channel capacities of the FSO and RF channels. A theoretical analysis on how this new technique can improve the performance of the system in terms of bandwidth utilization and system availability is presented.
- Introduction of Hybrid Channel Codes that can achieve the capacity of the hybrid FSO/RF channels. Hybrid Channel Codes provide more than two orders of improvement in terms of bit error rate and many orders of improvement in channel availability. The throughput obtained using Hybrid Channel Codes is also 35% better than the currently existing best systems.

- Hybrid Channel Codes provide a viable solution to many of the long standing problems on “last mile connectivity”, “broadband access to rural areas” and “disaster recovery”. As a broader application, these codes can be used in communication systems where there are two parallel channels with varied transmission and error rates.

1.2.2 Improved Decoding Algorithm on Channels with Memory

This thesis provides the following contributions in the areas of channels with memory.

- The thesis extends the improved decoding algorithm proposed earlier for memoryless channels to channels with memory.
- A density evolution analysis for the improved decoding algorithm on channels with memory is proposed.
- The improved decoding algorithm for channels with memory is further extended to ISI channels with AWGN noise (magnetic recording systems). It is found that the improved decoding technique can lead to over one dB gain for these channels which can lead to huge advantages in terms of storage densities for storage systems.

1.3 Outline of Thesis

This thesis is organized as follows. In chapter 2, hybrid FSO/RF communication systems is discussed. We discuss the potential applications of these systems and the problems faced in making their implementation a reality. A new mechanism that will considerably improve the performance of current communication systems is proposed. Novel error correction codes called “Hybrid Channel Codes” are then introduced which can be used to utilize both the FSO and the RF channels effectively. Results

that characterize the performance of the novel system and compare its usefulness to existing best systems are then presented.

Chapter 3 introduces the “guess algorithm” that has been proposed earlier for memoryless channels. This algorithm is then extended to channels with memory. It is then shown that the gains provided by the “guess algorithm” on channels with memory are greater than those obtained in memoryless channels. This is done using asymptotic analysis called density evolution. The improved decoding algorithm is then applied to magnetic recording systems (partial response channels) which are characterized by ISI and AWGN noise. Simulations results which show the benefits of this decoding method for storage systems are also presented.

Chapter 4 concludes the thesis and presents potential future work in the areas of hybrid communications and magnetic recording systems.

CHAPTER 2

HYBRID RF OPTICAL WIRELESS NETWORKS

2.1 Introduction

Free Space Optical (FSO) communication systems, also known as wireless optical communications, provide tremendous potential for low-cost time-constrained high-bandwidth connectivity in a variety of network scenarios. Several long-standing problems such as “last mile connectivity”, “broadband internet access to rural areas”, “disaster recovery” and many others can be solved using FSO communication systems. This is because, point-to-point line-of sight (LOS) FSO communication systems can achieve data rates comparable to fiber optics without incurring exorbitant costs and requiring significant amount of time for installation. However, the widespread deployment of FSO communication systems has been hampered by the reliability or availability issues related to atmospheric variations [33, 9]. FSO communication undergoes significant deterioration whenever the visibility in the medium is effected especially in cases smoke and fog. Another system that faces similar problems due to atmospheric conditions of precipitation such as rain and snow is the millimeter wave (MMW) system operating at 60 GHz. Consequently, both FSO and MMW communication systems fall short of the desired carrier-grade availabilities of 99.999%. Recently, several researchers and companies have suggested the idea of hybrid FSO/RF communication as a solution to the availability problem (see [22] and references therein). A low data-rate RF channel acts as a backup link to ensure minimum data communication when the main FSO link is down. Alternately, a high-data rate MMW channel duplicates the FSO link to create redundancy. These approaches

to hybridization provide viable solutions to the availability problem. However, the solutions are not efficient in terms of bandwidth utilization and usage of resources on both the channels. The objective of this thesis is to make hybrid FSO/RF communication systems achieve carrier class level (“five-nines”) reliabilities and still avoid the reduction in effective data rate due to data duplication. The truly hybridized system we propose can work when the effective SNR of the combined FSO/RF channel is higher than a threshold as opposed to earlier systems which work when the effective SNR of each of the individual channels is over a threshold. We propose a novel coding paradigm called “Hybrid Channel Coding” to achieve this goal. By avoiding data duplication, we preserve the crucial security benefit of the FSO communication system. In this system, the FSO and RF links dynamically interact with each other in order to achieve maximum reliability along with optimum utilization of channel resources leading to big improvements in performance in terms of system availability, bit error rates and effective channel throughput.

The rest of this chapter is organized as follows. Section 2.2 summarizes the previous work done in this direction. In Section 2.3, we provide an analytical comparison of existing systems with our proposed system in terms of system availability and average throughput obtained and show that the proposed scheme can lead to significant performance improvements. Section 2.4 provides the design of efficient error correction codes that can achieve the capacity of the hybrid FSO/RF channel irrespective of the underlying channel conditions. Simulation results that support our claims are present in Section 2.5.

2.2 Related Work

Recently, there has been growing interest in FSO for terrestrial communications and several companies [27, 13] are now offering commercial FSO communication products. An important issue with FSO communication systems is scintillation effect,

which leads to the loss of large amounts of data during transient bursts [34, 10]. Error control codes have been considered as a means for reducing the resulting bit errors [7, 58, 26, 37, 60]. Atmospheric fading in FSO channels can be modeled using a variety of distributions [59, 36, 56, 11]. The burst length in the atmospheric channel is found to be ranging from a few milliseconds to hours [56] making the channel highly unreliable. In order to reduce the coding redundancy during low and moderate scintillation, a rate adaptive coding scheme using variable length turbo codes has been proposed [25]. Interleaving along with error control coding can improve the code performance in case of small scale channel fluctuations [58]. However, system outages due to extreme conditions can make the link completely useless or reduce the range of transmission. In such situations, along with error control codes, range reduction using multiple hops can be used to increase channel availability [1]. However, this can lead to an increase in the expenditure on equipment and inefficient utilization of the system whenever the channel conditions become normal again. Diversity techniques can be used to improve channel utilization without any of the negative effects of interleaving or range reduction. Multiple copies of the same data can be transmitted using temporal [50, 23], spatial [23], coding [61, 46] or media [22] diversity. In temporal diversity, a delayed copy of the coded sequence is sent over the channel. Using multiple transmitters and/or receivers will lead to a spatially diverse system. With coding diversity, multiple copies of the same data are transmitted over the channel using space-time codes [46]. However, these diversity mechanisms can only help in case of short-term channel fluctuations. During extreme weather conditions, such as snow or fog, these mechanisms suffer from the same disadvantages as those using non-diversity schemes. One diversity scheme suitable for extreme climate conditions is media or channel diversity, which is the basis for hybrid FSO/RF communications. In this diversity scheme, a copy of the original message is sent over two heterogeneous parallel channels [57, 5]. In [22], the authors propose the use of a low-capacity RF

channel as a backup for the FSO link. The RF link is used only when the optical wireless channel is down. Another system makes use of a 60GHz MMW channel in conjunction with the FSO channel [22]. There are two reasons for such a combination. First, using MMW data transmission allows the RF link to achieve data rates comparable to that of the FSO link, i.e., over 1 Gbps. In this manner, the RF link does not merely act as a backup. Second, the two channels provide an optimum combination for high availability since MMW communication is mostly affected by rain while FSO communication suffers most in fog [22, 57, 5]. Redundancy in transmission over independent channels probabilistically improves the chances of message recovery at the receiver. Error control coding schemes can be used in these scenarios as well where media diversity helps mitigate the long term bursts and the error control coding helps reduce the bit error rates. However, we believe that the current approach to hybrid FSO/RF communication is highly inefficient and suffers from certain inherent problems. The duplication of data on the RF and FSO channels leads to the wastage of bandwidth and under-utilization of RF link whenever the FSO link is working normally. FSO communication is inherently secure because disruption of the link needs a direct obstruction of the point-to-point link. However, retransmission of the message over the insecure RF channel leads to an insecure communication system. Also, frequent switching between the FSO and RF links, called flapping [12], can lead to a collapse of the communication system. This undesirable behavior arises if the FSO and RF links become alternately unavailable for short periods of time. Moreover, the need for multiple encoders and decoders results in increased costs and synchronization issues. In this chapter, we introduce a new coding paradigm called “Hybrid Channel Coding” that utilizes both channels to the fullest to tackle the mentioned problems. “Hybrid Channel Codes” use the combination of non-uniform codes and rate-adaptive codes using only a single encoder and decoder to vary the code-rate based on the channel conditions. Media diversity in combination with non-uniform

codes is used to overcome long channel outages and rate-adaptivity is used to combat short term channel fluctuations. Additionally, the non-uniform codes used are of long block lengths that allow utilization of LDPC codes to their fullest potential. We show that true hybridization can be accomplished when both channels collaboratively compensate the shortcomings of each other and thereby, improve the performance of the system as a whole.

2.3 A Novel Hybrid FSO/RF System

In this part of the chapter, we present the channel model that is used for hybrid FSO/RF communication systems and present a novel hybrid FSO/RF mechanism developed in order to increase the system reliability.

2.3.1 Channel Model

The FSO channel is a highly unstable channel. Attenuation in FSO channel is caused due to absorption and scattering by the particles in the atmosphere [57]. Attenuation due to absorption is caused by atmospheric conditions and is dependent on the frequency of the transmitted wave. This includes attenuation due to visibility conditions such as fog, snow and rain. The transmitted light beam is also scattered in all directions due to the variations in particle size along the transmitted path. Apart from the attenuation and scattering losses due to the visibility conditions, the atmosphere also exhibits high amount of turbulence due to the variation of temperature and pressure. These variations in temperature and pressure create changes in the refractive index along the transmitted path leading to random intensity fluctuations. These random intensity fluctuations are termed as scintillation and are the major cause of outage in FSO channels. Scintillations in the optical channel are modeled using Kolmogorov theory [19]. It is important to note that severe scintillation and attenuation due to visibility conditions occur independently of each other. Severe

scintillation cannot occur during extreme visibility conditions (such as snow and fog) and vice versa.

The channel model defined here is similar to the one used in [2]. The FSO and RF channels can be modeled using (2.1) in which X denotes the transmitted binary signal, I denotes the instantaneous channel intensity gain, η the efficiency of the receiver aperture and $N \sim N(0, \frac{N_0}{2})$.

$$Y = \eta IX + N, I > 0. \quad (2.1)$$

The intensity I , is a random variable that varies as a gamma-gamma distribution ((2.2)) when the signal is passing through the FSO channel [51] and as a log-normal distribution ((2.3)) when passing through the RF channel (in case a backup RF channel exists).

$$f_I(z) = \frac{2(\alpha\beta)^{\frac{\alpha+\beta}{2}}}{\Gamma(\alpha)\Gamma(\beta)} z^{\frac{(\alpha+\beta)}{2}-1} K_{\alpha-\beta}(2\sqrt{\alpha\beta}z),$$

$$\alpha = \left(\exp \left[\frac{0.49\sigma_{FSO}^2}{(1+1.11\sigma_{FSO}^{\frac{5}{6}})^{\frac{7}{6}}} \right] - 1 \right)^{-1}, \quad (2.2)$$

$$\beta = \left(\exp \left[\frac{0.51\sigma_{FSO}^2}{(1+0.69\sigma_{FSO}^{\frac{5}{6}})^{\frac{5}{6}}} \right] - 1 \right)^{-1}.$$

$$f_{\tilde{I}}(z) = \frac{1}{2z\sigma_{RF}\sqrt{2\pi}} \exp -\frac{(\ln z)^2}{8\sigma_{RF}^2}. \quad (2.3)$$

Γ denotes the gamma function and $K_{\alpha-\beta}$ is a modified Bessel function of the second kind of order $\alpha - \beta$. σ_{FSO} and σ_{RF} are the parameters that indicate the scintillation strength in each of the channels respectively. The larger the value of σ

the more severe the scintillation. Other channel models such as the log-normal model also exist for modeling weak scintillations [24] in the FSO channel. However, the gamma-gamma model is a more accepted model for the entire range of scintillations (weak, moderate and strong). Typical values of scintillation index for σ_{FSO} are 0.5, 1.0 and 3.0 respectively for weak, moderate and strong scintillations. In this analysis, we do not include the attenuation due to the channel conditions and provide an analysis only on scintillation which is the main reason for channel unavailability in optical wireless communication systems.

2.3.2 Definitions and Notations

In this section, we specify some notations and definitions that are used in the rest of the analysis to follow. System availability is usually defined as the percentage of time the intensity of the received signal is above a threshold. Equivalently, we define the system availability as the percentage of time the capacity of the system is above a specified threshold. The capacity thresholds for the existing and the newly proposed systems are denoted as c_{Th} and $c_{\overline{Th}}$ respectively. Our definition of availability allows for a fair comparison of the earlier systems with the proposed system.

For the rest of the analysis, we assume that perfect channel state information is available both at the transmitter and the receiver as in [24], i.e. if the channel system states are $s = \eta I$, then the pdf of the channel states is $f_S(s) = \frac{1}{\eta} f_I(\frac{s}{\eta})$, where $f_I(i)$ is the probability density function of the intensity gain of the underlying channel (FSO or RF). With this assumption, the capacity of the optical wireless channel ($C_{FSO}(s)$) is the average capacity of an Additive White Gaussian Noise (AWGN) channel [60, 24]. We denote the capacity of the AWGN channel, dependent on the channel states (s) and the noise variance ($\frac{N_0}{2}$) as $C_{AWGN}(s, N_0)$. Similarly, we denote the capacity of the RF channel as $C_{RF}(\bar{s}, \bar{N}_0)$ where \bar{s} denotes the channel states and $\frac{\bar{N}_0}{2}$ denotes the noise variance of the RF channel. Let s_{Th} and $s_{\overline{Th}}$ denote the channel states at which

the capacities of the existing and the new systems are c_{Th} and $c_{\overline{Th}}$ respectively. Also, for a random variable X , the CDF (cumulative distribution function) is denoted by $F_X(x)$ and is equal to $Prob(X \leq x)$. The system availability is denoted by P_A .

2.3.3 Case 1: Fixed Rate Code on a Single FSO Link

This case can be considered as the base for the rest of the analysis to follow. A system with only the FSO channel and using a fixed rate code has the worst performance (in terms of throughput and channel availability) of all the systems considered. This is due to the lack of any mechanism to compensate for the losses incurred due to the channel variations. The burden of recovering from the channel losses falls completely on the coding mechanism used. Using a high rate code can be detrimental when the coding mechanism is unable to correct all errors. A low rate code would lead to a higher redundancy and bandwidth wastage. Using the definition stated earlier, the system availability is given by (2.4) and is analogous to that mentioned in [24]. The average throughput of the channel is given by the fixed rate of the code utilized and is given by (2.5). The code rate that will ensure minimum communication to be possible is therefore $C_{FSO}(s_{Th})$.

$$P_A = 1 - Prob(C_{FSO} \leq c_{Th}) = 1 - \int_0^{s_{Th_{FSO}}} f_S(s_{FSO}) ds_{FSO}, \quad (2.4)$$

$$\text{Avg. Throughput} = P_A(FSO) \times C_{FSO}(s_{Th_{FSO}}). \quad (2.5)$$

2.3.4 Case 2: Adaptive Rate Codes on a Single FSO Link

Using a code that adjusts its rate based on the channel conditions will enable the system to adaptively achieve a better performance by effectively improving the average throughput. The system availability, however, will remain the same as in

the case of having a fixed rate code (given by (2.4)). The average throughput is now given by (2.6).

$$\begin{aligned} \text{Avg. Throughput} &= P_A(FSO)E[C_{FSO}|\text{Available}] \\ &= P_A(FSO) \int_{s_{Th_{FSO}}}^{+\infty} \frac{C_{FSO}(s_{FSO})f_S(s_{FSO})}{1-F_S(s_{Th_{FSO}})} ds_{FSO}. \end{aligned} \quad (2.6)$$

2.3.5 Case 3: RF Backup Channel with a Fixed Rate Code

The RF channel can be used as backup in case the FSO link fails. The system availability in this case is given by (2.7) and the average throughput by (2.8). The states in the FSO and RF channels are denoted as s_{FSO} and s_{RF} respectively. $s_{Th_{FSO}}$ and $s_{Th_{RF}}$ denote the states at which the FSO and RF channels attain their respective threshold capacities.

$$\begin{aligned} P_A &= (1 - Prob(C_{FSO} \leq C_{Th_{FSO}})) + Prob(C_{FSO} \leq C_{Th_{FSO}}) \\ &\quad \times ((1 - Prob(C_{RF} \leq C_{Th_{RF}}))) \\ &= (1 - \int_0^{s_{Th_{FSO}}} f_{S_{FSO}}(s_{FSO}) ds_{FSO}) + \int_0^{s_{Th_{FSO}}} f_{S_{FSO}}(s_{FSO}) ds_{FSO} \\ &\quad \times (1 - \int_0^{s_{Th_{RF}}} f_{S_{RF}}(s_{RF}) ds_{RF}), \end{aligned} \quad (2.7)$$

$$\begin{aligned} \text{Avg. Throughput} &= [P_A(FSO)] \times C_{FSO}(s_{Th_{FSO}}) \\ &\quad + [1 - P_A(FSO)] \times [P_A(RF)] \times C_{RF}(s_{Th_{RF}}). \end{aligned} \quad (2.8)$$

2.3.6 Case 4: RF Backup Channel with Adaptive Codes

The situation can be further improved with an adaptive code which helps increase the channel throughput while the backup RF channel helps increase the system availability. The availability is again given by (2.7) as in Case 3. The average throughput, though, is higher than that obtained in the previous case and is denoted by (2.9).

$$\begin{aligned} \text{Avg. Throughput} &= [P_A(FSO)]E[C_{FSO}|\text{Available}] \\ &\quad + [1 - P_A(FSO)][P_A(RF)]E[C_{RF}|\text{Available}] \\ &= [P_A(FSO)] \int_{s_{Th_{FSO}}}^{\infty} \frac{C_{FSO}(s_{FSO})f_{S_{FSO}}(s_{FSO})}{1-F_{S_{FSO}}(s_{Th_{FSO}})} ds_{FSO} \\ &\quad + [1 - P_A(FSO)][P_A(RF)] \int_{s_{Th_{RF}}}^{\infty} \frac{C_{RF}(s_{RF})f_{S_{RF}}(s_{RF})}{1-F_{S_{RF}}(s_{Th_{RF}})} ds_{RF}. \end{aligned} \quad (2.9)$$

2.3.7 Case 5: Independent Parallel FSO/RF Channels with Adaptive Codes

In a system using independent parallel FSO/RF channels, data is transmitted over both the FSO and RF channels. However, this data transmission can occur in two different ways. In the currently existing systems, the parallel RF channel is used to repeat the data that is transmitted on the FSO channel. In such a system, there is no channel flapping. However, due to data repetition, the goodput obtained using this system is half the maximum possible.

The goodput can be increased considerably if the RF channel is also used for transmitting actual information and not repeat the data transmitted over the FSO channel. This, in itself, is a novel hybrid FSO/RF system. No mechanism currently exists that transmits information over both the channels without using the RF channel for repetition or as a backup. In this system, the two channels use separate rate-adaptive codes for each of the FSO and RF links, thus, requiring additional encoder decoder equipment expenditure.

The system availability for both the systems is the same and is equal to that in Case 3. However, the average throughput increases considerably over the system using the RF channel as a backup and is as shown in (2.10). The goodputs, as mentioned earlier, are however different.

$$\begin{aligned} \text{Avg. Throughput} = & [P_A(FSO)] \int_{sth_{FSO}}^{+\infty} \frac{C_{FSO}(s_{FSO})f_{s_{FSO}}(s_{FSO})ds_{FSO}}{1-F_{s_{FSO}}(sth_{FSO})} \\ & + [P_A(RF)] \int_{sth_{RF}}^{+\infty} \frac{C_{RF}(s_{RF})f_{s_{RF}}(s_{RF})ds_{RF}}{1-F_{s_{RF}}(sth_{RF})}. \end{aligned} \quad (2.10)$$

2.3.8 Case 6: Hybrid Channel Codes for Combined FSO/RF Channels

In this system, a single encoder decoder combination, using Hybrid Channel Codes, is used for the transmission of data. Hybrid Channel codes have two important properties compared to the coding and diversity mechanisms described earlier. First, the system is optimized on the sum of the capacities of both the channels combined

together (i.e. $C_{FSO} + C_{RF}$) instead of individual channel capacities C_{FSO} and C_{RF} . Hybrid Channel Codes try to achieve this combined channel capacity. Second, this method utilizes the properties of two important coding mechanisms: rate-adaptive and non-uniform. Rate-adaptive codes allow for the efficient usage of each of the FSO and RF channels. Non-uniform codes come with various advantages [42]. They enable the implementation of more efficient architectures for multiple channels using a single encoder and a single decoder. Moreover, they allow the usage of long block lengths which result in better error correction properties when used with LDPC codes. Also they provide better error floor performance. These properties lead to a further improvement in the availability which is shown in (2.11). c_{Th} here is the threshold for combined channel capacity. The average throughput obtained using Hybrid Channel Codes is also better than the previously mentioned schemes due to the effects of non-uniform codes. This, however, is not reflected in the (2.12) as the average throughput shown here is a theoretical limit. Nevertheless, simulations show that the Hybrid Channel Coding system yields the highest system availability and highest throughput of all the FSO/RF systems described. For (2.11) and (2.12), we define $C_{combined} = C_{RF} + C_{FSO}$ and s_{Th} as the state at which the capacity is c_{Th} .

$$\begin{aligned}
P_A &= 1 - Prob(C_{combined} \leq c_{Th}) \\
&= 1 - \int_0^{+\infty} \int_{s_{Th}-s_{FSO}}^{+\infty} f_{s_{FSO}}(s_{FSO}) f_{s_{RF}}(s_{RF}) ds_{RF} ds_{FSO}
\end{aligned} \tag{2.11}$$

$$\begin{aligned}
\bar{A} &= P_A \times E[C_{combined} | \mathbf{Available}] \\
&= P_A \int_0^{+\infty} \int_{s_{Th}-s_{FSO}}^{+\infty} C_{combined}(s_{FSO}, s_{RF}) \times f_{s_{FSO}}(s_{FSO}) \\
&\quad \times f_{s_{RF}}(s_{RF}) ds_{RF} ds_{FSO}
\end{aligned} \tag{2.12}$$

The availability analysis in this section can be represented using Figure 2.1. In the figure, the vertically shaded region represents the system availability for Cases 1 and 2 where there is only a single FSO channel. The system is available whenever the capacity is above the prescribed threshold of the FSO channel. It is clear from

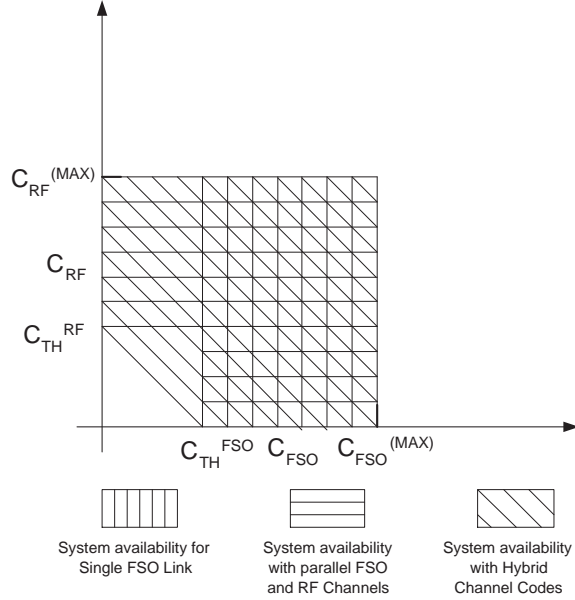


Figure 2.1. System availability for different optical wireless systems.

the figure that the system availability is increased considerably by using a backup RF channel. This is shown by the horizontally shaded area in the figure. This was discussed earlier in Cases 3, 4 and 5. The availability is further increased by using the Hybrid Channel Coding mechanism. This is the cross shaded area in the figure which represents Case 6. Notice that the advantages of Hybrid Channel Codes are not shown by the figure though it is still the best of all the systems presented. The figure only shows a theoretical overview of the advantages of the proposed system. The practical implications of using non-uniform codes which allow large block lengths and can provide advantages beyond those shown in the figure are not reflected and will become evident in the results section.

2.4 A Novel Coding Mechanism

The hybrid FSO/RF channel consists of two communication channels both of which are highly time-variant, as it was discussed in earlier sections. In order to

achieve efficient and reliable communication on the hybrid FSO/RF link we propose a novel coding paradigm, called *Hybrid Channel Codes*. This coding scheme is based on two important concepts: non-uniform (multi-channel) coding, and rate-compatible coding. Non-uniform codes were recently proposed in [43]. They provide a highly efficient and reliable communication scheme over several parallel channels using modern codes such as low-density parity-check (LDPC) codes. However, these codes are designed for the scenarios in which the channels are fixed, i.e., time-invariant. Rate-compatible LDPC codes have been shown to achieve close-to-capacity performance for highly time-variant channels using only one encoder and decoder [42, 41]. The main idea behind Hybrid Channel Codes is to combine non-uniform coding and rate-adaptive coding. These codes are introduced and analyzed, and we will design and optimize these codes for hybrid FSO/RF systems. Our results confirm that significant improvements in reliability and efficiency are obtained by using Hybrid Channel Codes.

2.4.1 Hybrid Channel Codes

Hybrid Channel Codes combine the advantages of non-uniform coding and rate-adaptive coding. Given the already established advantages of both techniques, this is a very promising scheme. The non-uniformity of the code is very effective in dealing with the bursty nature of the channels, while rate-adaptivity provides efficient utilization of the channels that are time-varying. Figure 2.2 depicts the structures of Hybrid Channel Codes. We use a very common graphical representation called Tanner Graph [48]. The Tanner Graph of a Hybrid Channel Code consists of five types of nodes as shown in Figure 2.2. Check nodes, RF variable nodes, FSO variable nodes, RF punctured nodes, and FSO punctured nodes. The number of RF and FSO variable nodes are n_{RF} and n_{FSO} , respectively. The block length of the code is equal to $n = n_{RF} + n_{FSO}$. The number of RF punctured nodes is given by np_{RF} , where

p_{RF} is the fraction of RF nodes that are punctured. Similarly, the number of FSO punctured nodes is given by np_{FSO} . Define, $\phi = \frac{np_{RF}}{n_{RF}}$ and $\psi = \frac{np_{FSO}}{n_{FSO}}$.

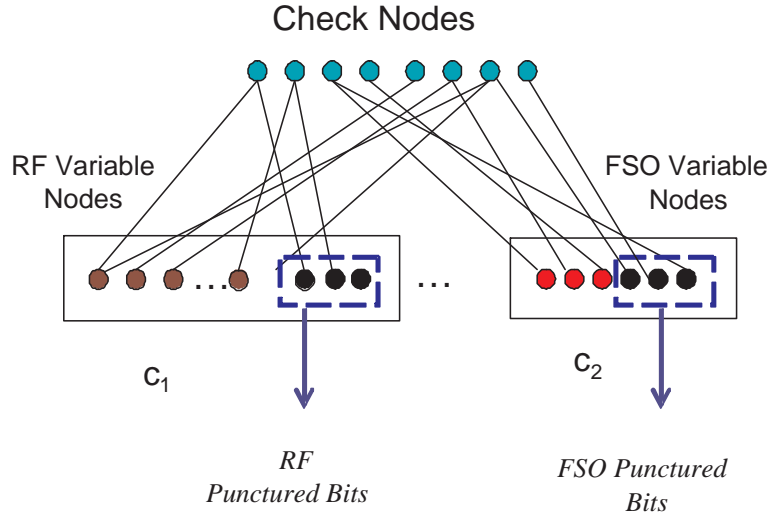


Figure 2.2. Graphical representation of Hybrid Channel Codes.

The punctured bits (bits corresponding to the punctured nodes) will not be transmitted. During decoding, the initial LLRs of the punctured nodes are set to zero. The percentage of punctured bits determines the code rate. It is assumed that the channel state information is available at the transmitter so that the percentage of punctured nodes can be adjusted accordingly. In the following sections, we provide analysis and design of these codes for efficient and reliable communication. In particular, we first show that Hybrid Channel Codes are capacity-achieving under maximum likelihood decoding. We then provide density evolution analysis to show their performance under iterative decoding and then provide the design of optimal Hybrid Channel Codes. We obtain the achievable rate regions for iterative decoding. Using the simulation results, we confirm that these codes provide efficient and reliable communication over hybrid FSO/RF channels. It should be mentioned that in our analytic results, we have assumed the two channels to be memoryless to keep the math manageable.

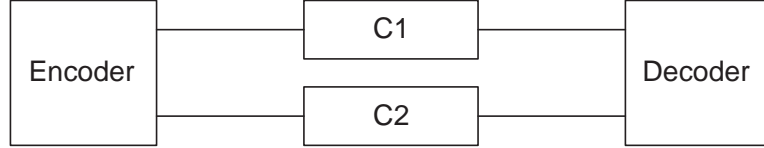


Figure 2.3. Hybrid Channel Coding architecture.

2.4.2 Optimality of Hybrid Channel Codes for Hybrid FSO/RF Channels

Here we state a fundamental result asserting that Hybrid Channel Codes are essentially optimal for hybrid FSO/RF systems. This result serves as a theoretical basis for our work. Consider two independent channels C_1 and C_2 that are used in parallel as shown in Figure 2.3. Suppose c_1 and c_2 are the capacities of the two channels respectively. Since the channels are independent, from an information theoretic point of view, the maximum achievable data rate using this system is $r_{max} = c_1 + c_2$. In our specific case of time-variant FSO/RF channels, c_1 and c_2 change over time and so does r_{max} . The main idea behind Hybrid Channel Coding is to achieve the data rate $r_{max} = c_1 + c_2$, independent of the channel conditions. That is, we want to achieve the highest possible data rate at any time. Clearly, no scheme can achieve higher rates than the mentioned scheme, since, this limit is imposed by information theory. We now state a result saying that Hybrid Channel Codes can achieve r_{max} at all times. This important result implies that only one encoder and decoder can be used to achieve the capacity of a highly time-variant hybrid channel. Note that, we have proved the result for maximum likelihood decoding. In practice, we use simple iterative decoding which has been shown, by simulation, to perform very close to maximum likelihood decoding for optimal codes.

Theorem 1. *Let C_1 and C_2 be two binary-input output-symmetric memory-less (BIOSM) channels, that are used in parallel as shown in Figure 2.3. Let α and β be two fixed real numbers in $(0,1)$. Assume the capacities of C_1 and C_2 at any time t is given by*

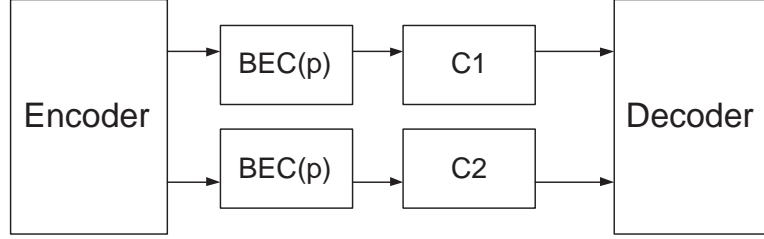


Figure 2.4. Proof of Theorem 1.

c_1 and c_2 , where $\alpha < c_1, c_2 < \beta$. There exists a Hybrid Channel Code that achieves the rate $r_{max}(t) = c_1(t) + c_2(t)$ at all times. This is done by proper puncturing and using maximum likelihood decoding at the receiver.

Proof. The theorem can be proved using conventional information theoretic proofs, however, we find the following proof interesting and short. Consider the case where the channel capacities are the minimum in the range we are studying. That is assume $c_1 = c_1^{min} \geq \alpha$, and $c_2 = c_2^{min} \geq \alpha$. Let $R_0 = \frac{c_1^{min} + c_2^{min}}{2}(1 - \epsilon)$. Note that here we assume the code rates and channel capacities are always between 0 and 1. Thus, capacity achieving codes have rates close to $\frac{c_1^{min} + c_2^{min}}{2}$. We construct an ensemble of LDPC codes suggested by MacKay [31], in which columns are constructed independently and randomly and they have weight t . The code rate is chosen to be R_0 . This code will be our parent code. As it is proved in [35], the ensemble can achieve the capacity of BIOSM channels. Thus for sufficiently large t , the error probability for any BIOSM channel with capacity smaller than R_0 can be made arbitrarily small.

Now assume that the channel conditions improve, and the capacities become c_1 and c_2 respectively. Let the puncturing fraction, p , be chosen as

$$p = 1 - \frac{c_1^{min} + c_2^{min}}{c_1 + c_2}. \quad (2.13)$$

The punctured bits are chosen randomly from the codeword bits. The interesting point is that this system can be modeled as the system shown in Figure 2.4. In this

figure, the puncturing effect is modeled by two binary erasure channels with erasure probabilities p . As it is shown in [35], the error rate is vanishing as long as the code rate is smaller than the capacity of the channel. The equivalent channel has the capacity:

$$c_{eq} = \frac{1}{2}[c_1(1-p) + c_2(1-p)] = c_1^{min} + c_2^{min}. \quad (2.14)$$

Thus the error probability goes to zero as t goes to infinity. But the code rate of the punctured code is given by

$$R = \frac{R_0}{1-p} = \frac{c_1 + c_2}{2}(1-\epsilon). \quad (2.15)$$

Thus we conclude all rates smaller than $\frac{c_1+c_2}{2}$ are achievable. Therefore, we can achieve the channel capacity at all times. It should be mentioned that we can also prove this theorem using a similar method to [17]. \square

This important result assures us that from a theoretical point of view, Hybrid Channel Codes are suitable for the hybrid FSO/RF systems. Note that the theorem assumes both channels to be memory-less. This assumption is used to simplify the analysis, though it is not always true. Nevertheless, the result is still good enough to encourage the use of Hybrid Channel Codes for our system. Interestingly, the Hybrid Channel Codes achieve optimal rates without any need for changing the encoder and the decoder. For example, even if one of the channels completely fails, i.e., the signal-to-noise ratio drops drastically; we still have reliable communication as long as the other channel has a good signal-to-noise ratio. In this case, we can simply shut off the corresponding transmitter without manipulating the encoder and the decoder. In fact, the decoder assumes that the unused channel has zero capacity. This versatility of the coding scheme is a significant advantage over existing FSO/RF systems, since, it avoids any problematic issues of switching between the two channels [12].

2.4.3 Density Evolution

Here, we provide density evolution formulas to analyze the performance of Hybrid Channel Codes under iterative decoding. Assume that the RF and the FSO channels are memory-less binary-input output-symmetric (MBIOS) channels. Let γ_{RF} and γ_{FSO} be the the signal to noise ratios (SNR) of the RF and FSO channels respectively. The SNRs show the channel conditions and depend on the signal intensity and the noise level. We assume that γ_{RF} and γ_{FSO} are real numbers in $[0, +\infty]$. Thus $\gamma = +\infty$ refers to the perfect channel conditions and $\gamma = 0$ refers to the case where the channel capacity is zero. For the RF channel, assuming the all-one code word has been sent, we define the random variable $Z_{\gamma_{RF}}$ as the log likelihood ratio of the transmitted bits, given that the SNR is γ_{RF} . Let $F_{RF}(z, \gamma_{RF})$ and $f_{RF}(z, \gamma_{RF})$ be the cumulative distribution function (CDF) and the probability density function (PDF) of $Z_{\gamma_{RF}}$ respectively. Similarly, define $Z_{\gamma_{FSO}}$, $F_{FSO}(z, \gamma_{FSO})$ and $f_{FSO}(z, \gamma_{FSO})$.

Consider Figure 2.3 where we transmit data over two independent binary-input output-symmetric channels, the RF and the FSO channels. Suppose, we use a Hybrid Channel Code of length n . We transmit any codeword over the two channels such that n_{RF} bits in any codeword are transmitted over the RF channel and n_{FSO} bits are transmitted over the FSO channel, so $n = n_{RF} + n_{FSO}$. Let E be the set of edges in the graph and let E^{RF} and E^{FSO} be the set of edges that are incident with variable nodes corresponding to the RF and FSO channels respectively. Also let E_i^{RF} be the set of the edges that are adjacent to the RF variable nodes of degree i . We define

$$\lambda^{RF}(x) = \sum \lambda_i^{RF} x^{i-1} \quad (2.16)$$

where

$$\lambda_i^{RF} = \frac{|E_i^{RF}|}{|E^{RF}|}. \quad (2.17)$$

Also, define $\lambda^{FSO}(x)$ accordingly. Let $\rho(x) = \sum \rho_i x^{i-1}$, where ρ_i is the fraction of edges connected to a check node of degree i [18]. Similar to [18], we can find the

density evolution formulas for the Hybrid Channel Codes ensemble. Let us define $q^{RF} = \frac{|E^{RF}|}{|E|}$ and $q^{FSO} = \frac{|E^{FSO}|}{|E|}$. Let P_l^{RF} denote the probability density function of the messages that are sent from RF variable nodes in the l th iteration of the message passing decoding. Define P_l^{FSO} accordingly. Then, the formulas for the density evolution can be written as

$$P_0^{RF}(x) = \phi\delta(x) + (1 - \phi)f_{RF}(x, \gamma_{RF}),$$

$$P_0^{FSO}(x) = \psi\delta(x) + (1 - \psi)f_{FSO}(x, \gamma_{FSO}),$$

$$P_l^{RF} = P_0^{RF} \otimes \lambda^{RF} \left(\Gamma^{-1} [\rho(\Gamma(\sum q^{RF} P_{l-1}^{RF}))] \right), \quad (2.18)$$

$$P_l^{FSO} = P_0^{FSO} \otimes \lambda^{FSO} \left(\Gamma^{-1} [\rho(\Gamma(\sum q^{FSO} P_{l-1}^{FSO}))] \right). \quad (2.19)$$

where \otimes denotes convolution and Γ is as defined in [18]. These results are obtained by applying the density evolution analysis of non-uniform codes [43], and punctured codes [42] to the Hybrid Channel Code ensemble. We can use these formulas to optimally design Hybrid Channel Codes. The simulation result will confirm the effectiveness of the design methodology.

2.4.4 Achievable Rate Region for Iterative Decoding

Here we provide achievable regions for Hybrid Channel Codes. In other words, we provide an exact characterization of the achievable puncturing patterns for a given Hybrid Channel Code ensemble. This is very useful because we can determine the achievable rates and these can be used in the design of efficient codes. We say that a puncturing pair $[p_{RF}, p_{FSO}]$ is achievable for an ensemble of Hybrid Channel Codes if there exists a $\gamma_{RF} < +\infty$ and $\gamma_{FSO} < +\infty$ such that a randomly chosen code from the ensemble can be used to achieve arbitrarily small error rate over the hybrid FSO/RF channel with SNRs γ_{RF} and γ_{FSO} . Otherwise, the pair $[p_{RF}, p_{FSO}]$ is not achievable.

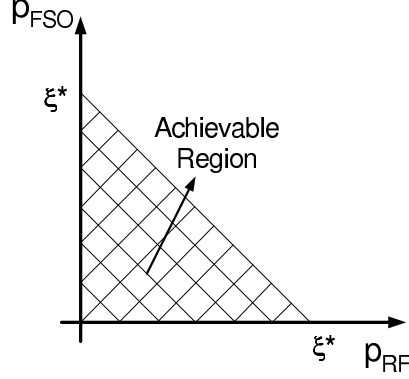


Figure 2.5. The achievable region for the puncturing pair $[p_{RF}, p_{FSO}]$.

Theorem 2. For an ensemble of Hybrid Channel Codes, define

$$x_0(\zeta) = 1, \quad x_l(\zeta) = \lambda(1 - \rho(1 - \zeta x_{l-1})), \quad \text{for } l = 1, 2, \dots \quad (2.20)$$

Let ζ^* be the maximum value for which $\lim_{l \rightarrow \infty} x_l(\zeta^*) = 0$. The puncturing pair $[p_{RF}, p_{FSO}]$ is achievable if and only if $p_{RF} + p_{FSO} < \zeta^*$.

Proof. Assume $p_{RF} + p_{FSO} > \zeta^*$. Define

$$y_0(\zeta) = 1, \quad y_l(\zeta) = \lambda(1 - \rho(1 - (p_{RF} + p_{FSO})y_{l-1})). \quad (2.21)$$

then $y_l(\zeta)$ is the fraction of erasure messages in the l^{th} iteration from the punctured variable nodes, assuming the noise level of the channels are zero. Then, we have $\lim_{l \rightarrow \infty} y_l > 0$. This means, even if the noise levels of the RF and FSO channels are zero, the punctured bits are not recovered at the decoder. Thus, the pair $[p_{RF}, p_{FSO}]$ is not achievable.

Now assume $p_{RF} + p_{FSO} < \zeta^*$. Thus, there exists an $\epsilon > 0$ such that $p_{RF} + p_{FSO} + 2\epsilon < \zeta^*$. The assumption $\lim_{l \rightarrow \infty} x_l(\zeta^*) = 0$ means that if the noise levels of the RF and FSO channels are zero and $p_{RF} + p_{FSO} = \zeta^*$, then all the punctured bits will be recovered during decoding. Thus, by increasing the noise level by a small amount and decreasing the puncturing fractions by ϵ (thus obtaining the pair $[p_{RF} + \epsilon, p_{FSO} + \epsilon]$) the error rate will still tend to zero. Thus, $[p_{RF}, p_{FSO}]$ is achievable. \square

The achievable region for Hybrid Channel Codes is shown in Figure 2.5.

2.5 Performance Results

In this section, we present results confirming our claims presented earlier in the thesis. Simulations are performed to observe the effects of Hybrid Channel Codes on channel utilization, bit error rates and channel availabilities.

2.5.1 Simulation Setup

To optimally compare the performance of various coding mechanisms in the varying channel conditions, we use the topology shown in Figure 2.6. We assume the existence of separate FSO and RF channels in a parallel topology. The FSO channel is assumed to have a bandwidth of 1 Gbps and the RF channel is assumed to have a bandwidth of 100 Mbps, giving a total channel capacity of 1.1 Gbps. A channel is assumed to be unavailable whenever its capacity falls below 10% of the initial value. In all the simulations performed, we assume the lack of any retransmission mechanism. This is done in order to compare the efficiencies of the coding schemes used. We also assume that a synchronization mechanism exists at the receiver to combine the data received from both the channels.

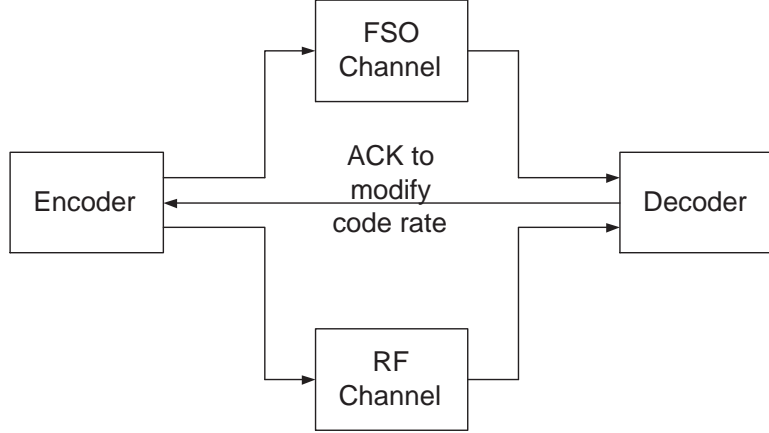


Figure 2.6. Simulation setup.

2.5.2 Results

2.5.2.1 Comparison of Channel Utilization for Various Coding Schemes

For this set of simulations, we assume that the FSO and RF channels are in one of three possible conditions: *good* (low noise variance), *medium* and *bad* (high noise variance). The simulation duration can be assumed as different days of a week when the atmospheric channel conditions are varying randomly. Good channel conditions indicate low scintillation index whereas bad channel conditions are simulated using a large scintillation index.

The three channel conditions allow nine different fading levels for the combined FSO and RF channels. As mentioned earlier, a log-normal fading model for the RF channel and the gamma-gamma fading model for the FSO channel is assumed. The channel conditions can be varied by varying the channel parameter (σ_{RF} and σ_{FSO} respectively). Table 2.1 shows the various parameters used. Note that the channel conditions here indicate the effects of scintillation during an extended period of time.

Table 2.1. Simulation parameters used for various channel conditions.

Channel	Good	Medium	Bad
σ_{RF}	0.25	0.5	1
σ_{FSO}	0.5	1	3

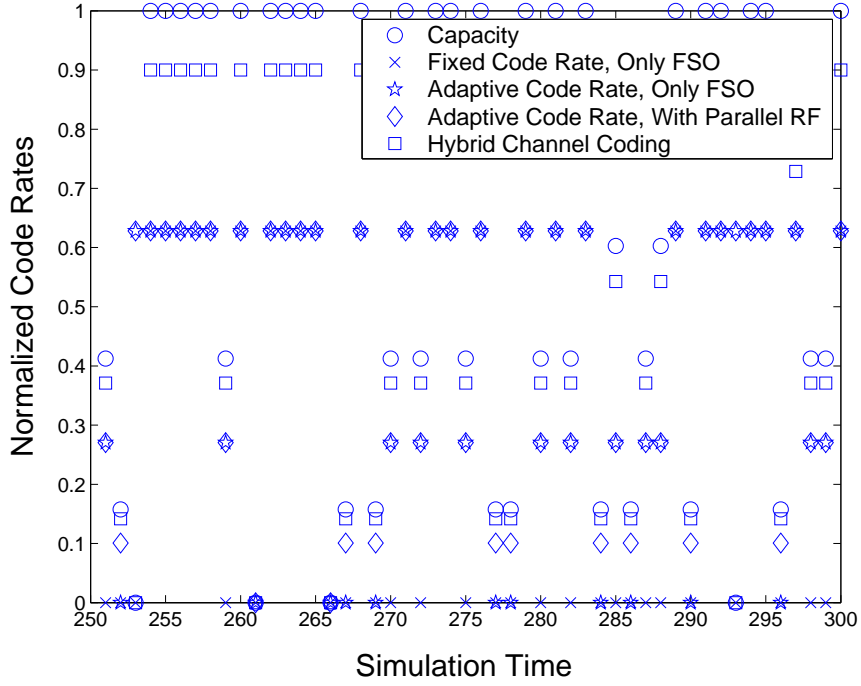


Figure 2.7. Code rate variation for different FSO/RF systems.

Figure 2.7 provides a “snapshot” of the variation of code rates, based on the channel conditions, for the different systems. The figure, thus, displays the effectiveness of the coding mechanism in utilizing the channel resources and achieving the combined channel capacity.

For a single FSO link with a fixed rate code, a fair throughput is obtained in good channel conditions provided the code used is of high rate. However, with a low rate code, the channel utilization is low. This system is unavailable for other channel conditions. The fixed rate code is generated using the irregular LDPC code shown in (2.22) [16]. The block length was set to 11390. The code used is found to produce good rate-adaptive codes with rates between 0.5 and 0.9. [16]. We choose the fixed code rate to be 0.7.

$$\lambda(x) = 0.25105x + 0.30938x^2 + 0.00104x^3 + 0.43853x^9, \quad (2.22)$$

$$\rho(x) = 0.63676x^6 + 0.36324x^7.$$

Using an adaptive code with the single FSO link leads to a more efficient channel usage in terms of throughput. In the figure, the same code as in (2.22) is used to generate rate-adaptive codes (using puncturing). A backup RF channel will aid in the increase of system availability. The RF channel, in this case, is used whenever the FSO channel is out. The system is unavailable whenever both the channels are unavailable. However, as is evident from the Figure 2.7, the system availability increases considerably over one using only a single FSO link. The channel utilization, in terms of throughput, improves when rate-adaptive codes are used on both the FSO and RF channels.

Using Hybrid Channel Codes results in the best performance. The usage of non-uniform codes enables longer effective block lengths. As shown in Figure 2.7, the rate of the codes obtained using Hybrid Channel codes closely follows the capacity curves. The average throughput, therefore, obtained using this technique is the highest among all the other existing schemes.

For the set of simulations shown in Figure 2.7, we found that the average throughput of the Hybrid Channel Coding system increases by five times over a system using a single FSO link and a fixed code rate. The average throughput is increased by more than 35% when compared to the system which uses independent parallel FSO/RF channels with rate-adaptivity and data duplication which is the currently existing best system. It needs to be stressed here that the goodput values obtained by using Hybrid Channel codes are much higher because of the elimination of data repetition. The goodput values that are obtained for various systems are shown in Table 2.2. These values are averaged for 100 runs of the simulation.

Table 2.2. Comparison of goodputs (in Gbps)obtained for various FSO systems.

Single FSO Link (Fixed Rate)	Single FSO Link (Adaptive Rate)	Parallel RF (Independent)	Hybrid Channel Codes
0.1975	0.2103	0.7224	1.0032

2.5.2.2 Comparison of System Availability

In this section, we compare the system availability probabilities of following three systems: one using a single FSO link with a fixed rate code, the second system using independent parallel FSO and RF channels and the third system using Hybrid Channel Codes. As mentioned in Section III, the system availability increases considerably when using our new coding mechanism as shown in Table 2.3. From the table, it is also clear that having the parallel RF channel increases the availability considerably for various capacity thresholds. However, the availability is further reduced when Hybrid Channel Codes are used. The normalized capacity threshold used in the simulations for both the channels is set to the same value. For example, in the Table 2.3, normalized capacity threshold of 0.1 means $c_{Th} = 0.1$ and $c_{\overline{Th}} = 0.1$. For this set of simulations, moderate scintillation indices in both the FSO and RF channels were assumed. In particular, $\sigma_{FSO} = 1.0$ and $\sigma_{RF} = 0.5$.

Table 2.3. Comparison of channel availability for combined and independent FSO/RF systems.

Normalized Threshold	% Availability (single FSO link) (Fixed Rate)	% Availability (independent) (Parallel FSO and RF)	% Availability (Hybrid Channel) (Codes)
0.05	76.4631	99.8056	99.9999
0.1	68.5543	98.4285	99.9999
0.15	63.2153	95.7741	99.9993
0.2	59.1518	92.2846	99.9955

2.5.2.3 Comparison of Bit Error Rates for various Coding Schemes

In this section, we compare the bit error rates (BER) of the currently existing coding mechanism using independent parallel channels with our mechanism using

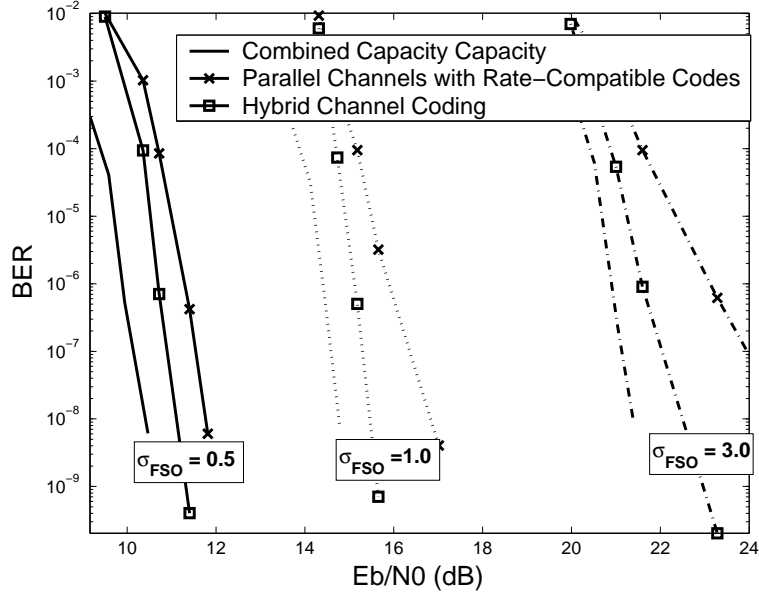


Figure 2.8. BER performance of different optical wireless systems.

Hybrid Channel Codes. The results are shown in Figure 2.8. The energy per bit for each of the coding mechanisms is calculated as the weighted average of the energy per bit in the two channels. The weights used for averaging are the channel bandwidths. We can see that, Hybrid Channel Codes result in over two orders of improvement in BER. This is due to media diversity and longer effective block lengths that are possible by the use of non-uniform codes. A system using independent parallel channels with rate-adaptive coding cannot take advantage of the longer effective block lengths.

A block length of 11390 is chosen for the FSO channel. For the RF channel the block length was chosen to be 1139 when using independent parallel channels with rate adaptive codes. The block length in case of using Hybrid Channel Codes is the sum of the block lengths on the FSO and RF channels i.e. 12529. This is because, we wish to keep the same latency constraints (assuming that both channels are transmitting at the same bit rate) for both the systems being compared. For the comparison, we choose three values of σ_{FSO} to denote three different scintillation conditions as mentioned in Table 2.1. For each of the three conditions, the capacity curves are also

shown. It can be seen from the figure that the Hybrid Channel Coding mechanism gets to within a dB of the capacity curve even at bit error rates of 10^{-8} .

We also observe that the penalty of keeping the second link always available is not too high when using Hybrid Channel Codes and proves to be an advantage along with the other benefits mentioned earlier. For a σ_{FSO} and σ_{RF} of 1.0 and 0.5 respectively, we obtain better bit error performance when using both the channels as opposed to using only a single link as can be seen in Figure 2.8.

2.6 Broader Impacts

The currently proposed novel system using Hybrid Channel Codes is not restricted in usage to only hybrid FSO/RF communication systems. It can also be extended to any systems that have parallel non-uniform channels. As the Internet is growing towards the Global Information Grid where multiple networks are combined to form a single “big” network, we can always apply such a scheme to improve the performance of communication systems using non-uniform parallel links. However, identifying such scenarios is important and will be a part of future work.

CHAPTER 3

IMPROVED DECODING ALGORITHM ON CHANNELS WITH MEMORY

3.1 Introduction

The capacity of many channels of interest has been achieved practically using LDPC codes [44]. An important advantage of using LDPC codes is the ease of their decoding. LDPC codes use an iterative message exchange based decoding algorithm called belief propagation (BP) decoder [49]. However, the iterative decoding is not always successful and its performance is inferior to Maximum Likelihood (ML) decoding, especially for short and moderate length codes. Improvements to the standard iterative decoder have been suggested independently in [40] and [52].

Recently, LDPC codes have been constructed to achieve the independent and uniformly distributed (i.u.d.) capacity of partial response (PR) channels [21, 20]. These channels are characterized by intersymbol interference (ISI) and additive white Gaussian noise (AWGN). A recent work by Kavcic et al. derives the performance bounds for an ensemble of LDPC codes using density evolution [20]. An important type of PR channel is the magnetic recording channel.

Due to the insatiable and ever-increasing needs of data storage, novel techniques have to be developed to improve the capacity of magnetic recording channels. These capacity requirements translate to improving storage densities and using higher recording rates. Coding and signal processing has been recognized as an important way to increase the storage densities [54]. Due to the high complexities involved in gaining additional storage density advantages, it needs to be emphasized that gains of even

a tenth of a dB translate into a highly effective system. Therefore, codes with a high rate that provide very low bit error rates (BERs) are necessary. In this thesis, we first extend the improved decoding mechanism proposed in [40] to ISI channels with AWGN. We then show through analysis and simulations that the improved decoding algorithm is much more effective when applied to these channels and can yield gains of over a dB. These gains translate to an advantage in storage density and have applications in improving the capacity of magnetic recording systems. The newly proposed system has slightly higher decoding complexity than the standard iterative belief propagation decoder.

The rest of the chapter is organized as follows. In Section 3.2, we briefly review the improved decoding algorithm and much of the past work done in this direction. Sections 3.3 and 3.4 extend the improved decoding algorithm to ISI channels and provide density evolution for the improved decoding method. In section 3.5, we apply the proposed “improved decoding algorithm” to magnetic recording channels and provide simulation results.

3.2 Related Work

LDPC codes work with sparse parity check matrices [14, 32]. The dependencies between the nodes in the LDPC codes are represented using bipartite Tanner graphs [49]. The fraction of edges originating from the variable and check nodes are represented using polynomials $\lambda(x)$ and $\rho(x)$ as shown in (3.1) and (3.2). d_v and d_c are the maximum degrees of variable and check nodes and λ_k and ρ_k denote the percentage of nodes that are connected to degree k variable and check nodes respectively. LDPC codes exhibit a threshold effect which is calculated using “density evolution” [28]. This helps in designing optimum codes which use simple linear time belief propagation decoding.

$$\lambda(x) = \sum_{k=1}^{k=d_v} \lambda_k x^{k-1} \quad (3.1)$$

$$\rho(x) = \sum_{k=1}^{k=d_c} \rho_k x^{k-1} \quad (3.2)$$

However, belief propagation decoding is inferior to ML decoding. To improve the performance of the belief propagation decoding to ML decoding, we introduced the “guess algorithm” [40] for memoryless channels. A similar work was introduced independently by Varnica et al [52]. Both these algorithms work once the belief propagation decoder fails. For the rest of the chapter, the names “guess algorithm” and “improved decoder” are used alternatively and refer to algorithm in [40]. The improved decoder is based on the assumption that a subset of the undecoded bits when guessed correctly can complete the decoding process successfully. Guessing the undecoded bits implies guessing the log-likelihood ratios (LLRs) of variable nodes that lead to decoding failure. These nodes can be chosen randomly from the set of all variable nodes. However, it has been shown in [40] that a more careful choice of variable nodes will drastically reduce the number of additional iterations required for successful decoding. [40] shows that by guessing 5 or 6 variable nodes that are connected to the maximum number of unsatisfied check nodes, the bit error rates can be reduced by a couple of orders of magnitude for memoryless channels while keeping the decoding complexity within reasonable limits.

Considerable research has been done to find the capacity of an ISI channel and design suitable LDPC codes for them [3, 55]. In particular, it has been shown that the capacity of a binary ISI channel is lower bounded by the capacity of binary channel with identically and uniformly distributed (i.u.d) input. LDPC code constructions using a new density evolution technique have been suggested in [47], [20] and refer-

ences therein. A partial response (PR) channel is a binary input continuous output AWGN channel characterized by ISI.

The magnetic recording channel is represented as a PR channel [54] and can be represented mathematically using (3.3), where Y_t is the received output, X_t is the encoded input modulated using BPSK and N_t is AWG noise, all at time t . h_k represents the coefficients of the ISI channel of length I .

$$Y_t = \sum_{k=0}^{k=I} h_k X_{t-k} + N_t \quad (3.3)$$

One important PR channel is the duobinary channel ($h(D) = (1 - D)/\sqrt{2}$). The joint code-channel graph of the LDPC code on ISI channel is shown in Figure 3.1(b) [20]. The iterative decoding over the PR channel is as shown in figure 3.1(a). The decoding process consists of two steps. The BCJR decoder [4] performs turbo equalization and passes the LLRs to the LDPC decoder. The LDPC decoder then performs the regular iterative decoding on the received LLRs. For additional BCJR iterations, extrinsic information is passed back by the LDPC decoder. In this thesis, we apply the improved decoding to the ISI channels and analyze its performance. We use simulations to prove the correctness of our analysis.

An improved decoding algorithm for channels with memory has been proposed in [53]. However, we need to stress here that we take a different approach than the one in [53]. In this thesis we provide density evolution analysis for the improved decoder over ISI channels and extend it to various applications for magnetic recording systems.

3.3 Improved Decoding Algorithm for ISI Channels

The BCJR equalization algorithm is generally used for decoding over ISI channels. Since the BCJR process is computationally expensive, methods have been suggested

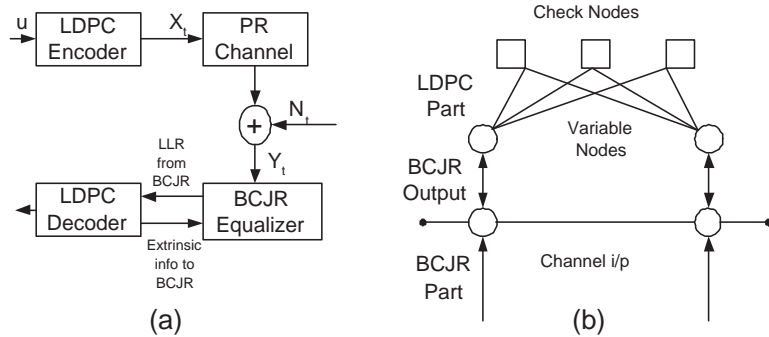


Figure 3.1. Block Diagram of PR channel

to reduce the decoding complexity [20] by using other iterative decoders in conjunction with the equalization step. The BCJR step is therefore, sometimes, performed only once for a number of iterations of the LDPC belief propagation decoding. Since the belief propagation decoding is not always as effective as ML decoding, we can use the “guess algorithm”, in this case also, to improve performance on ISI channels. Intuitively, the “guess algorithm” performs better on ISI channels than on memoryless channels because of dependencies of the guessed bits (due to channel memory). Once a bit is guessed correctly, the correct value propagates to the subsequent steps of the decoding process. We use density evolution analysis to support our intuition. We first explain how the improved decoding works on ISI channels.

Once the belief propagation decoder fails, variable nodes connected to the maximum number of unsatisfied check nodes are identified. The values of the top g of these variable nodes are set to saturation values ($+\infty$ or $-\infty$) and the decoding process is restarted. If decoding is successful, the bit error rates are reduced. However, if decoding fails, the values of the guessed bits are changed (guessed as another value) and the decoding process is restarted. Though these additional steps lead to increased number of iterations ($constant \times 2^g$), we obtain much better performance than using standard belief propagation decoding without guessing.

3.4 Density Evolution on ISI Channels

In this section, we provide density evolution analysis for the improved decoding algorithm on ISI channels. We need to stress here that density evolution is an asymptotic analysis where “guessed nodes” are chosen randomly. However, in practical implementations the “guessed nodes” are chosen more carefully leading to better gains than those obtained using density evolution. The density evolution steps for the standard iterative decoding process over the ISI channel are provided in [20] and are summarized as follows.

Suppose m_{cv} and m_{vc} denote the messages exchanged between the check nodes and variable nodes and vice versa. Suppose the probability density function (pdf) of the exchanged messages in the l^{th} round of the message passing decoder be denoted as f_{check}^l and f_{var}^l respectively. Also let the pdf of the apriori messages that are input to the channel trellis be denoted as $f_{apriori}^l$. Then the density evolution steps for the ISI channel are as shown in the (3.4). Similar to [20], a Monte-Carlo simulation was performed to obtain the pdf of the messages coming out of the channel trellis denoted by the operation T . $\bar{\lambda}$ denotes the averaging done with respect to the nodes rather than the edges.

$$\begin{aligned}
 f_{check}^l &= \rho(f_{var}^l) & (3.4) \\
 f_{apriori}^l &= \bar{\lambda}(f_{check}^l) \\
 f_{trellis}^l &= T(f_{apriori}^l, f_N) \\
 f_{var}^{l+1} &= f_{trellis}^l \otimes \lambda(f_{check}^l)
 \end{aligned}$$

The density evolution steps for the improved decoding algorithm on memoryless non-uniform channels was proposed in [39] and are shown in (3.5).

$$\begin{aligned}
f_{check}^{kl} &= \rho(f_{var}^l) \\
f_{var}^l &= \sum q^k f_{var}^{kl} \\
f_{var}^{k(l+1)} &= f_{var}^{k0} \otimes \lambda(f_{check}^{kl})
\end{aligned} \tag{3.5}$$

In (3.5), k denotes the channel through which the messages are received in the l^{th} round of the message passing decoding. q^k denotes the fraction of edges in the Tanner graph that are incident through channel of type k . f_{var} denotes the sum of the pdf of the messages coming from each channel. f_{var}^{k0} denotes the initial LLR of the received messages on channel k . In order to use density evolution analysis for improved decoding on ISI channels, we assume that the channel can be split into two independent channels: on one channel which is assumed to be perfect, the guessed bits are transmitted. The second is an ISI channel with AWGN through which the remaining bits are transmitted. This is shown in Figure 3.2. This assumption of non-uniform channels allows us to apply density evolution analysis on a set of parallel channels with different capacities. When the assumption of non-uniform channels as shown in Figure 3.2 is applied to ISI channels, the initial LLR of the messages will change. With improved decoding, the pdf of the received LLRs is no longer Gaussian as in the case of standard iterative decoding and has a peak at one end of the density function based on the guessed value ($+\infty$ or $-\infty$). The magnitude of the peak($\delta(x)$) is equal to the percentage of guessed nodes. Using this modification and the steps in (3.5), noise thresholds for various LDPC codes using the improved decoder can be obtained.

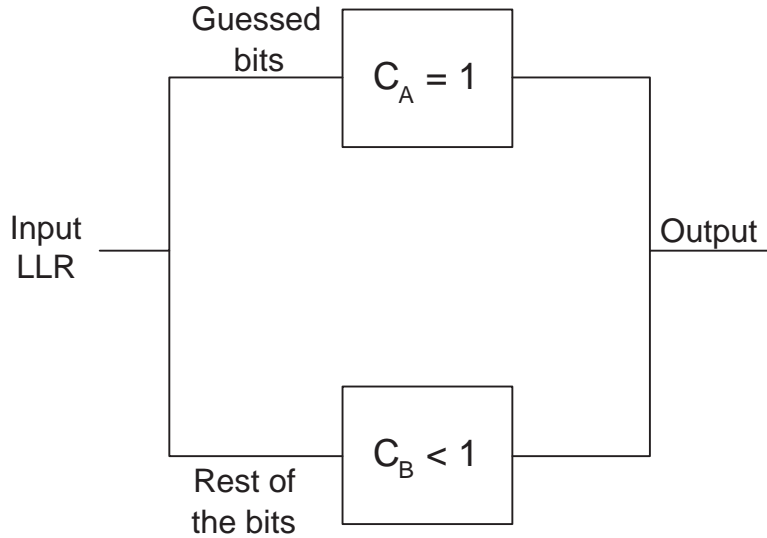


Figure 3.2. Equivalent channel for the improved decoding.

3.5 Simulation Results

Using analysis from previous sections, we implement density evolution for a set of $(3, X)$ regular LDPC codes whose variable node degree is 3 and the regular degree of check nodes is X . We use discretized density evolution algorithm for memoryless AWGN channels as mentioned by Chung et. al. [8]. In order to implement density evolution for the guess algorithm, we assume that 1% and 2% of the variable nodes are available for guessing. For a code of length 1000, 1% and 2% of nodes constitute 10 and 20 nodes respectively. We limit our “guesses” to 2% in the density evolution analysis because the maximum number of bits guessed in practical implementations is always much smaller.

We implemented density evolution for the dicode channel as described in [20] and extended it to include the improved decoding. The results are as shown in Tables 3.1 and 3.2. The tables show the noise thresholds obtained in the density evolution for different percentages of guessed bits as compared to the noise thresholds when not using the improved decoding algorithm. A higher noise threshold indicates better

performance in noise of the decoding algorithm. From the tables, it is clear that the improved decoding algorithm over channels with memory provides higher noise thresholds than those obtained over memoryless channels. This better performance is represented as gain in dB in the tables. The improved decoding algorithm performs better due to the dependencies introduced by the channel. Once a bit is guessed correctly, the decoder propagates the correct value as the iterations progress. This channel dependency cannot be used for advantage in memoryless channels. However, we need to emphasize that the gains obtained in actual implementations are always much higher even when the number of guessed bits is smaller. The improved decoding algorithm can be used to increase capacity of storage devices by using these channel dependencies. We need to stress here that characterizing this gain in terms of the code rate has not yet been done and is a problem of future research. For example, the gains obtained using a (3,15) regular code using density evolution are more than the gains obtained using a (3,60) regular LDPC code but smaller than a (3,150) regular LDPC code. However, this does not represent a repeated pattern and is different for different codes of the same rates.

Encouraged by the theoretical results for ISI channels, we implement the improved decoding algorithm over the magnetic recording channels. We use a regular (3,6) LDPC code and an irregular code with degree distribution as shown in (3.6) for this set of simulations. The irregular code has been optimized for a block length of 1000. The guessed nodes are selected using the constraints mentioned in [38].

$$\lambda(x) = 0.1212x + .6364x^2 + 0.2424x^5 \tag{3.6}$$

$$\rho(x) = 0.3818x^5 + 0.5939x^6 + 0.0243x^7$$

For this implementation, we use only 6 guesses. The additional number of iterations needed to complete the decoding successfully then reduces to 64. The results are as shown in Figure 3.3. It is clear from the figure that the “guess algorithm” provides better bit error rate performance than standard belief propagation. This translates

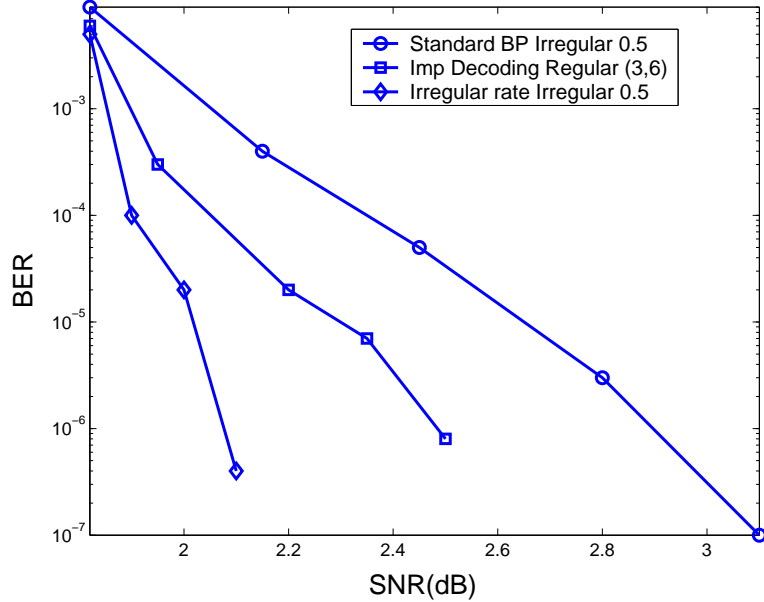


Figure 3.3. Improved performance using the guess algorithm for block length 1000 on a dicode channel.

to an SNR gain of about 0.4dB at a bit error rate of 10^{-6} for the (3,6) regular code and over a dB with the optimized irregular code respectively. This code has been optimized for a memoryless AWGN channel. It is also clear that the improvements obtained are better in the practical implementation than when using density evolution due to the reasons mentioned earlier. For the current scenario of magnetic recording channels, the maximum block length is limited by the sector length and is < 4100 unlike in density evolution analysis where asymptotic block lengths are assumed. Also, as expected, the results are better when irregular LDPC codes are used. The results in Tables 3.1 and 3.2 also confirm that the SNR gains increase as the degree of the check nodes is increased. In both density evolution analysis and in simulations, the (3,150) regular LDPC code provides gains of over a dB with the improved decoding algorithm. This is especially important in magnetic recording applications using high rate codes (rates ≥ 0.7). We also find that the performance of the improved decoding algorithm is better as the number of guessed nodes increases. But this increase in

number of guessed bits can lead to a prohibitive increase in the number of additional iterations to complete the decoding. The most important fact to be stressed here is that the gains obtained by the improved decoder on channels with memory are much higher than that obtained when it is used over memoryless channels. Simulations in [40] show that the improved decoding provides only about 0.5 dB gain in the best case with an optimized irregular LDPC code.

Table 3.1. Density evolution analysis of improved decoding over AWGN channels.

Code	σ	1%		2%	
		σ	in dB	σ	in dB
(3,3)	2.118576	2.118576	0	2.118576	0
(3,5)	1.009141	1.022026	0.1102	1.022281	0.1123
(3,6)	0.880639	0.902235	0.2108	0.902673	0.2150
(3,15)	0.563018	0.583574	0.3114	0.589541	0.3992
(3,60)	0.429864	0.446747	0.3345	0.451896	0.4341
(3,150)	0.374273	0.392164	0.4054	0.401665	0.6135

Table 3.2. Density evolution analysis of improved decoding over ISI channels with AWGN.

Code	σ	1%		2%	
		σ	in dB	σ	in dB
(3,3)	2.039851	2.039851	0	2.03986	0
(3,5)	0.945102	0.975346	0.2805	0.976155	0.2807
(3,6)	0.821685	0.861328	0.4093	0.869644	0.4927
(3,15)	0.547171	0.587646	0.6198	0.593414	0.7046
(3,60)	0.404344	0.427979	0.4934	0.430881	0.5521
(3,150)	0.354872	0.399985	1.04	0.402144	1.08

We find that the improved decoding algorithm performs better for codes of longer lengths also. In particular, a (3,6) code of length 4096 provides a gain of 0.5dB over the standard iterative decoder. The irregular LDPC code chosen in (3.6), however, does not show marked improvement over the regular code because it is not optimized for the longer length (4096). The results are shown in Figure 3.4.

We extended our algorithm to *EPR4* channel and find that the improvements are significant in these channels also as shown in Figure 3.5. From the figure, it is evident

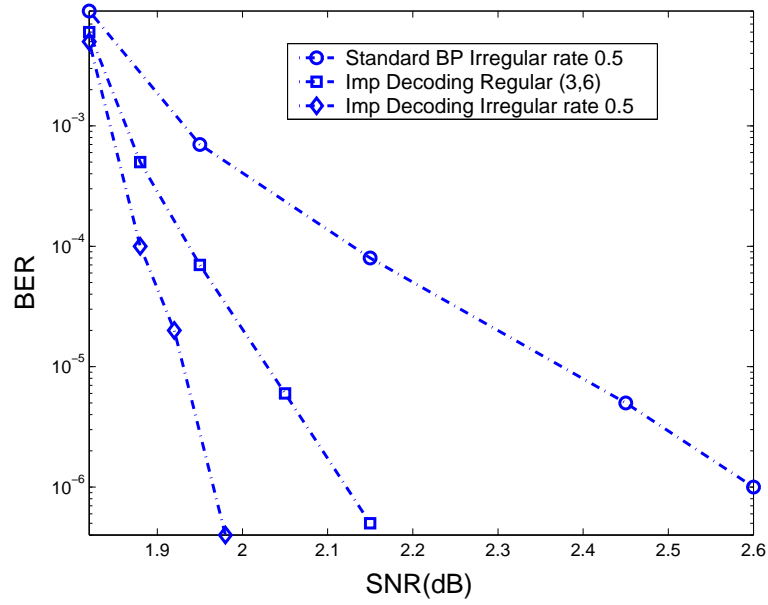


Figure 3.4. Improved performance using the guess algorithm for block length 4096 on a dicode channel.

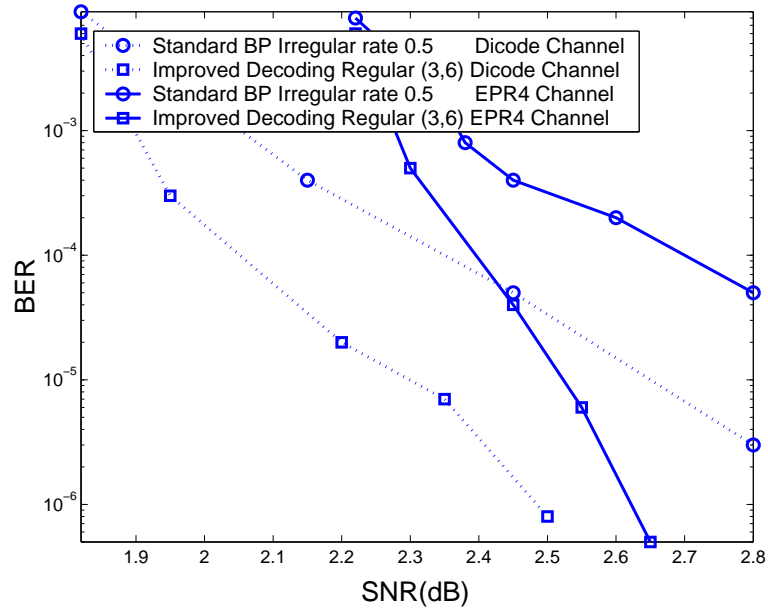


Figure 3.5. Improved performance using the guess algorithm for various PR channels for block length 1000.

that the improved decoding provides a gain of 1dB when using the regular (3,6) code for the *EPR4* channel at a bit error rate of 10^{-6} . From our results, it is evident that the improved decoding algorithm is better on channels with memory and gains provided by this algorithm on the magnetic recording channels are also significant. The *EPR4* channel is represented as shown in 3.7.

$$h_{EPR4}(D) = (1/2) * (1 - D + D^2 + D^3) \quad (3.7)$$

3.6 Summary and Future Work

In this chapter, it has been proved that an application of the “guess algorithm” to channels with memory yields better gains than those obtained on memoryless channels. These gains can be efficiently utilized to applications for magnetic recording systems. In particular, we can obtain gains of one dB on these PR systems. We used asymptotic density evolution analysis to prove our theory. However, the block lengths of magnetic recording systems are bounded by the sector length and finite length analysis will be more appropriate for these systems. In this case, pseudo-codeword analysis is needed and can be a good starting point for continuation of this thesis.

CHAPTER 4

CONCLUSIONS

In this thesis, important improvements have been suggested for two important communication systems: the hybrid FSO/RF system and the magnetic recording system. To both these systems, improvements have been suggested by the usage of efficient error correcting codes that can improve the system performance in terms of availability, bit error performance and throughput.

One of the biggest problems with the hybrid FSO/RF communication systems that hamper their practical use is their inability to provide 99.999% reliability. In this thesis, we suggest a novel hybrid FSO/RF technique that, unlike previous systems, utilizes both the FSO and RF channels effectively and increases system availability. The proposed novel system is a combination of media diversity mechanism proposed earlier that utilizes novel codes that can achieve the combined channel capacity of the FSO and the RF channels. We then design optimal codes, termed Hybrid Channel Codes, to achieve this combined channel capacity. These codes use non-uniform, rate-adaptive LDPC codes that in conjunction with the media diversity scheme can provide excellent performance improvements over the currently existing best systems. Simulation results are provided to show that the new system proposed is better in terms of system availability, bit error rate performance and channel utilization (throughput and goodput). This thesis provides an excellent starting point for the implementation of a system that can solve many of the long standing issues of last-mile connectivity and disaster recovery. Future work can include the imple-

mentation of Hybrid Channel Codes using efficient VLSI architectures and a testbed to compare the performance of the proposed system to that of existing systems.

In the second part of the thesis, an improved decoding algorithm, called the “guess algorithm” proposed earlier for memoryless channels has been extended to channels with memory. Asymptotic density evolution analysis is then provided to show that the improved decoding algorithm provides bigger gains over these channels with memory. These codes are then applied to magnetic recording systems that are characterized by intersymbol interference (ISI) with AWGN noise. Using simulations, the new decoding algorithm is found to produce over a dB gain for magnetic recording systems which are translated to an huge advantages in terms of the area of the storage device. An important restriction on the implementation of LDPC codes in this devices is the block length which is restricted by the sector size of the storage device being used. Typical block lengths of these devices do not exceed 5000 bits. A good extension for this work will be finite length analysis of this improved decoding algorithm. Pseudo-codeword analysis will be a good starting point.

BIBLIOGRAPHY

- [1] Akella, J., Yuksel, M., and Kalyanaraman, S. Error analysis of multi-hop free-space optical communication. In *IEEE ICC 2005* (May 2005), pp. 1777–1781.
- [2] Anguita, J. A., Djordjevic, I. B., Neifeld, M. A., and Vasic, B. V. High-Rate Error-Correction Codes for the Optical Atmospheric Channel. In *SPIE 2005* (August 2005), pp. 58920V1–58920V7.
- [3] Arnold, D., and Loeliger, H. On the Information Rate of Binary-Input Channels with Memory. In *IEEE International Conference on Communications (ICC), Vol.9* (June 2001), pp. 2692–2695.
- [4] Bahl, L.R., Cocke, J., Jelenik, F., and Raviv, J. Optimal Decoding of Linear Codes for Minimizing Symbol Error Rate. *IEEE Transactions on Information Theory* (March 1971).
- [5] Bloom, S., and Hartley, W. The Last-mile Solution: Hybrid FSO Radio. Whitepaper, AirFiber Inc., May 2002.
- [6] Chae, S., and Park, Y. Low Complexity Encoding of Improved Regular LDPC Codes. In *IEEE 60th Vehicular Technology Conference* (September 2004), pp. 2535– 2539.
- [7] Chan, V. Coding for the Turbulent Atmospheric Optical Channel. *IEEE Transactions on Communications* 30, 1 (1982), 269–275.

- [8] Chung, S.Y., Forney, G.D., Richardson, T.J., and Urbanke, R. On the Design of Low-Density Parity-Check Codes within 0.0045 dB of the Shannon Limit. *IEEE Communications Letters* 5, 2 (February 2001).
- [9] Clark, P., and Sengers, A. Wireless Optical Networking: Challenges and Solutions. In *MILCOM 2004* (October 2004), pp. 416–422.
- [10] David, F. Scintillation Loss in Free-Space Optic IM/DD Systems. In *Free Space Laser Communication Technologies XVI, SPIE 2004* (January 2004), pp. 65–75.
- [11] Doss-Hammel, S., E.Oh, Ricklin, J.C., Eaton, F.D., Gilbreath, G.C., and Tsinikidis, D. A Comparison of Optical Turbulence Models. In *SPIE 2004* (August 2004), pp. 236–246.
- [12] FreeSpaceOptics. Free space optics: Informational website. <http://www.freespaceoptic.com/>.
- [13] fSONA. Free-Space Optical Networking Architecture. <http://www.fsona.com>.
- [14] Gallager, R. G. Low-Density Parity Check Codes. *IRE Trans. Inform. Theory* Vol. IT-8 (January 1962), 21–28.
- [15] Gallager, R. G. *Low-density Parity-Check Codes*. Cambridge, MA: MIT Press, 1963.
- [16] Ha, J., and McLaughlin, S.W. Optimal Puncturing of Irregular Low-density Parity-check Codes. In *IEEE International Conference on Communications (ICC)* (May 2003), pp. 3110–3114.
- [17] Hsu, C., and Anastasopoulos, A. Capacity Achieving LDPC Codes through Puncturing. In *International Conference on Wireless Networks, Communications and Mobile Computing* (2005), pp. 1575–1580.

- [18] J. Richardson, T., Shokrollahi, M. A., and Urbanke, R. L. Design of Capacity-approaching Irregular Low-density Parity-check Codes. *IEEE Transactions on Information Theory* 47 (2001), 619–637.
- [19] Karp, S., Gagliardi, R., Moran, S.E., and Scotts, L.B. *Optical Channels*. Plenum, MA, 1988.
- [20] Kavcic, A., Ma, X., and Mitzenmacher, M. Binary Intersymbol Interference Channels: Gallager Codes, Density Evolution and Code Performance Bounds. *IEEE Transactions on Information Theory* 49, 7 (July 2003), 1636–1652.
- [21] Kavcic, A., Ma, X., and Varnica, N. Matched Information Rate Codes for Partial Response Channels. *IEEE Transactions on Information Theory* 51, 3 (March 2005).
- [22] Kim, I. I., and Korevaar, E. Availability of Free Space Optics (FSO) and Hybrid FSO/RF Systems. In *Optical Wireless Communications IV* (August 2001).
- [23] Lee, E.J., and Chan, V. Part 1: Optical Communication over the Clear Turbulent Atmospheric Channel Using Diversity. *IEEE Journal on Selected Areas in Communications* 22, 9 (2004), 1896–1906.
- [24] Li, J., and Uysal, M. Optical Wireless Communications: System Model, Capacity and Coding. In *IEEE 58th Vehicular Technology Conference (VTC 2003-Fall)* (October 2003), pp. 168–172.
- [25] Li, J.T., and Uysal, M. Achievable Information Rate for Outdoor Free Space Optical Communication with Intensity Modulation and Direct Detection. In *IEEE GLOBECOM 2003* (November 2003), pp. 2654–2658.

- [26] Li, J.T., and Uysal, M. Error Performance Analysis of Coded Wireless Optical Links over Atmospheric Turbulence Channels. In *IEEE Wireless Communications and Networking Conference (WCNC)* (March 2004).
- [27] LightPointe. Lightpointe Communications. <http://www.lightpointe.com/home.cfm>.
- [28] Luby, M., Mitzenmacher, M., Shokrollah, A., and Spielman, D. Analysis of Low Density Codes and Improved Designs using Irregular Graphs. In *Thirtieth annual ACM symposium on Theory of computing* (1998), pp. 249–258.
- [29] Luby, M.G., Mitzenmacher, M., Shokrollahi, M.A, and Spielman, D.A. Efficient erasure correcting codes. *IEEE Transactions on Information Theory* 47 (2001), 569–584.
- [30] Luby, M.G., Mitzenmacher, M., Shokrollahi, M.A, and Spielman, D.A. Improved low-density parity-check codes using irregular graphs. *IEEE Transactions on Information Theory* 47 (2001), 585–598.
- [31] MacKay, D .J. C. Good Error-correcting Codes Based on Very Sparse Matrices. *IEEE Transactions on Information Theory* 45 (1999), 399–431.
- [32] MacKay, D.J.C., and Neal, R.M. Near Shannon Limit Performance of Low-Density Parity-Check Codes. *Electron. Lett.* 32 (August 1996), 1645–1646.
- [33] Mahdy, A., and Deogun, J. S. Wireless Optical Communications: A Survey. In *IEEE Wireless Communications and Networking Conference (WCNC)* (March 2004), pp. 2399–2404.
- [34] Majumdar, A. K., and Ricklin, J. Effects of the Atmospheric Channel on Free-Space Laser Communications. In *SPIE 2005* (August 2005), pp. 58920K1–58920K16.

- [35] Miller, G., and Burshtein, D. Bounds on the maximum likelihood decoding error probability of low density parity check codes. *IEEE Transactions on Information Theory* 47 (2001), 2696–2710.
- [36] Muhammad, S.S., Kohldorfer, P., and Leitgeb, E. Channel Modeling for Terrestrial Free Space Optical Links. In *IEEE ICTON 2005* (July 2005), pp. 407–410.
- [37] Navidpour, S.M., Uysal, M., and Kavehrad, M. Performance Bounds for Correlated Turbulent Free-Space Optical Channels. In *CERS 2006* (March 2006).
- [38] Pishro-Nik, H., and Fekri, F. Improved decoding algorithms for low-density parity-check codes. In *3rd International Symposium on Turbo Codes and Related Topics* (2003), pp. 117–120.
- [39] Pishro-Nik, H., and Fekri, F. Results on Non-uniform Error Correction Using Low-Density Parity Check Codes. In *IEEE Globecom* (December 2003), pp. 2041–2045.
- [40] Pishro-Nik, H., and Fekri, F. On Decoding of Low-Density Parity-Check Codes over the Binary Erasure Channel. *IEEE Transactions on Information Theory* 50, 3 (March 2004), 439–454.
- [41] Pishro-Nik, H., and Fekri, F. On Raptor Codes. In *IEEE International Conference on Communications (ICC)* (2006).
- [42] Pishro-Nik, H., and Fekri, F. Results on Punctured Low-density Parity-check Codes and Improved Iterative Decoding Techniques. *IEEE Transactions on Information Theory* 53 (2007), 599–614.
- [43] Pishro-Nik, H., Rahnavard, N., and Fekri, F. Non-uniform Error Correction Using Low-density Parity-check Codes. *IEEE Transactions on Information Theory* 51 (2005).

- [44] Richardson, T. J., and Urbanke, R. L. The capacity of low-density parity-check codes under message-passing decoding. *IEEE Transactions on Information Theory* 47 (2001), 599–618.
- [45] Shannon, C. E. A Mathematical Theory of Communication. *Bell System Technical Journal* 27 (1948), 379423.
- [46] Simon, M., and Vlnrotter, V.A. Alamouti-Type Space-Time Coding for Free-Space Optical Communication with Direct Detection. *IEEE Transactions on Wireless Communications* 4, 1 (2005), 35–39.
- [47] Song, H., Kumar, B.V.K.V., Kurtas, E., Yuan, Y., McPheters, L.L., and McLaughlin, S.W. Iterative Decoding for Partial Response (PR), Equalized, Magneto-Optical (MO) Data Storage Channels. *IEEE Journal on Selected Areas in Communications* 19, 4 (April 2001).
- [48] Tanner, R. M. A Recursive Approach to Low Complexity Codes. *IEEE Transactions on Information Theory* 27 (1981), 533–547.
- [49] Tanner, R. M. A Recursive Approach to Low Complexity Codes. *IEEE Transactions on Information Theory IT-27* (September 1981), 533547.
- [50] Trisno, S., Smolyaninov, I.I., Milner, S., and Davis, C. C. Characterization of Time Delayed Diversity to Mitigate Fading in Atmospheric Turbulence Channels. In *SPIE 2005* (July 2005), pp. 5892151–58921510.
- [51] Uysal, M., J.Li, and Yu, M. Error Rate Performance Analysis of Coded Free-Space Optical Links over Gamma-Gamma Atmospheric Turbulence Channels. *IEEE Transactions on Wireless Communications* 5, 6 (2006), 1229–1233.
- [52] Varnica, N., and Fossorier, M. Belief-propagation with Information Correction: Improved Near Maximum-Likelihood Decoding of Low-Density Parity-Check

- Codes. In *International Symposium on Information Theory (ISIT)* (June 2004), p. 343.
- [53] Varnica, N., Fossorier, M., and Kavcic, A. Augmented Belief-Propagation Decoding of Low-Density Parity-Check Codes. *IEEE Transactions on Communications* 54, 10 (October 2006).
- [54] Vasic, B., and Kurtas, E.M. *Coding and Signal Processing for Magnetic Recording Systems*. CRC Press, NY, 2004.
- [55] Vontobel, P.O., and Arnold, D.M. An Upper Bound on the Capacity of Channels with Memory and Constraint Input. In *IEEE Information Theory Workshop (ITW)* (September 2001), pp. 147–149.
- [56] Wilfert, O., and Kolka, Z. Statistical Model of Free-Space Optical Data Link. In *SPIE 2004* (August 2004), pp. 203–213.
- [57] Wu, H., Hamzeh, B., and Kavehrad, M. Achieving Carrier Class Availability of FSO Link via a Complementary RF Link. In *38th Asilomar Conference on Signals, Systems and Computers, Vol.2* (November 2004), pp. 1483–1487.
- [58] Y.T.Koh, and Davidson, F. Interleaved concatenated coding for the turbulent atmospheric direct detection optical communication channel. *IEEE Transactions on Communications* 37, 6 (1989), 648–651.
- [59] Zhu, X., and Kahn, J. M. Free-space optical communication through atmospheric turbulence channels. *IEEE Transactions on Communications* 50, 8 (2002), 1293–1300.
- [60] Zhu, X., and Kahn, J. M. Performance Bounds for Coded Free-Space Optical Communications through Atmospheric Turbulence Channels. *IEEE Transactions on Communications* 51, 8 (2003), 1233–1239.

- [61] Zhuang, Z., Ma, D., and Wei, J. Diversity Coding Scheme for Wireless Optical Communication with Direct Detection. *IEE Electronics Letters* 40, 13 (2004).